Transport Limitations in Thermal Diffusion

Nicholas Cox, Pawel Drapala, and Bruce F. Finlayson
Department of Chemical Engineering, University of Washington, Seattle, WA, USA

Abstract

Numerical simulations are made of thermal field flow fractionation (TFFF) to illustrate and quantify transport effects in experiments. In TFFF, molecular diffusion and thermal diffusion compete to create a concentration gradient in an otherwise uniform concentration field. In any flow device there are entrance regions in which the velocity and temperature profile are developing. Thus, interpretation of data is clouded by the fact that the temperature gradient is not established over the total region of flow. The magnitude of such errors is determined for flow devices described in the literature.

In a thermal diffusion cell, used to measure the Soret coefficient, the ratio of the thermal diffusion coefficient to the molecular diffusion coefficient, the profile is developed over some time. A macroscopic model provides guidance about the time to reach steady state.

The same phenomenon is relevant in the experiments by Braun and Libchaber (1). In this experiment, a thin cylinder of fluid containing DNA is heated by a laser along the centerline. Convection is created through a gravitational force, and a temperature gradient is established. This temperature gradient then provides a driving force for thermal diffusion, which causes the DNA to increase in concentration near the center and bottom of the cylinder. Simulations show the same behavior as seen experimentally.

Introduction

Thermal diffusion is the phenomenon whereby mass flux occurs due to a temperature gradient in addition to a concentration gradient. In thermal flow field fractionation, a temperature gradient is imposed perpendicular to the flow direction and this causes a concentration gradient perpendicular to the flow direction, too. Commonly the flow is between two flat plates, in laminar flow, and the velocity is a maximum in the center and zero at the wall. Thus, the molecules moved vertically by the thermal diffusion and mass diffusion move into regions having different velocities. Thereby separation occurs because different molecules have different diffusion and thermal diffusion coefficients.

The theory is based upon equations from deGroot and Mazur (2). The mass flux of component one is given by (2-4)

$$j_1 = -\rho D \nabla c - \rho D_T c(1-c)\nabla T$$

where j_1 is the mass flux, ρ is the density of the solution, D is the diffusion coefficient of the solute in the solvent, c is the mass fraction of the solute (component 1) in the solvent (component

2), D_T is the thermal diffusion coefficient, and T is the temperature. If the solute is dilute, this reduces to

$$j_1 = -\rho D \nabla c - \rho D_T c \nabla T$$

Dividing by the average molecular weight of the mixture (assumed constant in a dilute system) converts this to molar flux.

If the solution is placed between two flat plates that are held at different temperatures, creating a linear temperature profile in the vertical direction, the dilute equation reduces to

$$\frac{D_T}{D}\frac{dT}{dx} = -\frac{1}{c}\frac{dc}{dx}$$

But $dT/dL = \Delta T/L$, where L is the thickness between the plates. This can be integrated to give the concentration distribution vertically.

$$c(x) = c(0)\exp\left[-\frac{x}{L}\frac{D_T}{D}\Delta T\right]$$

This is the solution for an infinite domain. When the domain is finite (as it has to be) it is necessary to solve for $c(0)$, which is done to maintain a specified average concentration. A key parameter is the thermal diffusion coefficient, D_T, or the Soret coefficient, $S_T \equiv D_T/D$. Data is available (3-5). Several theories exist to predict the Soret coefficient (4, 6, e.g.) but there is yet no agreement on the proper theory. For these parameters and ΔT=10ºC, $c(0) = 1.85c_{avg}$; for ΔT=100ºC, $c(0) = 14c_{avg}$. An important aspect of the numerical calculations is the necessity of keeping the average concentration fixed in a closed vessel.

In this work we use typical dimensions of devices from Janca (7): plates 76 mm long, 0.1 mm apart, with a temperature difference top to bottom of 10 ºK. With temperature ranges of 10-100 ºK, Giddings (5) indicates polymer molecules can be separated with molecular weights ranging from 10^4 to 10^7. We numerically solve the equations of motion, the energy equation, and a diffusion equation with the thermal diffusion terms added. The Soret coefficient is taken as 0.14 K^{-1}, which is a typical value and the value measured by Braun and Libchaber for DNA. We also simulate the convection, diffusion, and thermal diffusion of DNA, as done experimentally by Braun and Libchaber (1).

TFFF with Flow

The geometry is shown in Figure 1. The equations governing fluid flow, energy transport, and thermal and mass diffusion in steady state are:

$$\rho \mathbf{u} \bullet \nabla \mathbf{u} = -\nabla p + \eta \nabla^2 \mathbf{u},$$
$$\rho C_p \mathbf{u} \bullet \nabla T = k \nabla^2 T,$$
$$\mathbf{u} \bullet \nabla c = \nabla \bullet [D \nabla c + D_T c \nabla T]$$

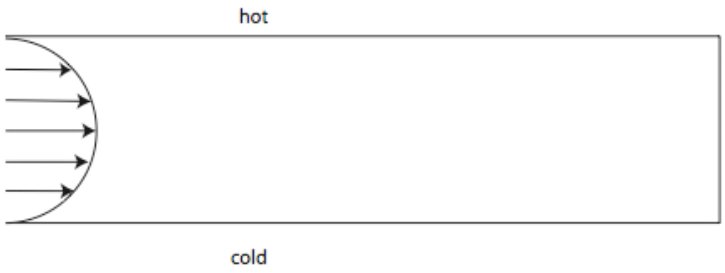

Figure 1. Thermal field flow fractionation

where **u** is the velocity, p is the pressure, η is the viscosity, C_p is the heat capacity, and k is the thermal conductivity. The equations are solved in Comsol Multiphysics® by using the Navier-Stokes equation, the energy equation, and a General PDE equation in the form

$$-\nabla \bullet \Gamma = 0, \quad \Gamma = -D \nabla c - D_T c \nabla T + \mathbf{u} c$$

The boundary conditions are no slip on the top and bottom walls, temperatures of 308 ºK an 298 ºK on the top and bottom wall, respectively, no mass flux on the top and bottom wall, specified velocity at the inlet, and a constant concentration (mole fraction) of solute at the inlet. The specified average velocity was 0.13 ms^{-1} and the profile was either parabolic or constant. The inlet temperature was either 298ºK or a linear profile corresponding to the energy flux. Outlet conditions were flow conditions. The parameters were $D = 10^{-11}$ m^2s^{-1}, $S_T = 0.14$ K^{-1}, $\rho = 998$ kgm^{-3}, $\eta = 0.001$ Pa s, k = 0.609 $Wm^{-1}K^{-1}$. Under these conditions the Reynolds number was 13, which is in the laminar regime. This problem was solved using the Comsol Multiphysics program using 45,824 quadrilateral elements (due to the long device with a small aspect ratio) and 402,489 degrees of freedom. The mesh was finer near the inlet (see Figure 2). The velocity was solved first (in a few minutes on a Macintosh G5 computer); then the temperature and concentration were solved together, using the velocity just found.

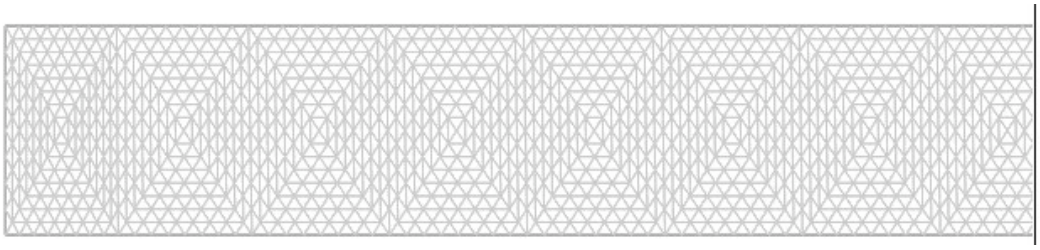

Figure 2. Finite element mesh for entry portion of TFFF (shown 0.1 mm high, first 1 mm long)

When the inlet velocity profile is parabolic (fully developed) but the temperature is uniform at the temperature of the lower plate, it takes some distance for the temperature to develop into a constant vertical gradient. The temperature very near the inlet is shown in Figure 3. The temperature along the centerline, halfway between the plates, is shown in Figure 4, and it has reached its asymptotic value within 7.5 mm, or within 10% of the total length. The mass fraction profile at the outlet is shown in Figure 5 and shows that the thermal diffusion is causing the solute to redistribute, but it hasn't completely done so in 76 mm. A similar picture of the outlet concentration occurs when the temperature at the inlet is a linear profile so that the temperature gradient is constant throughout the entire length. Thus, while the temperature redistributes at the inlet, it has only a very small effect on the concentration distribution out the device. If the velocity is taken as a flat profile, it reaches the fully developed profile (parabolic) within 0.1 mm, or approximately a length equal to the height between the plates. Thus, velocity rearrangement at the inlet is also unimportant.

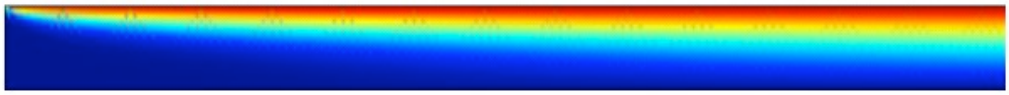

Figure 3. Temperature near inlet of TFFF (red = 308, blue = 298, first 1 mm)

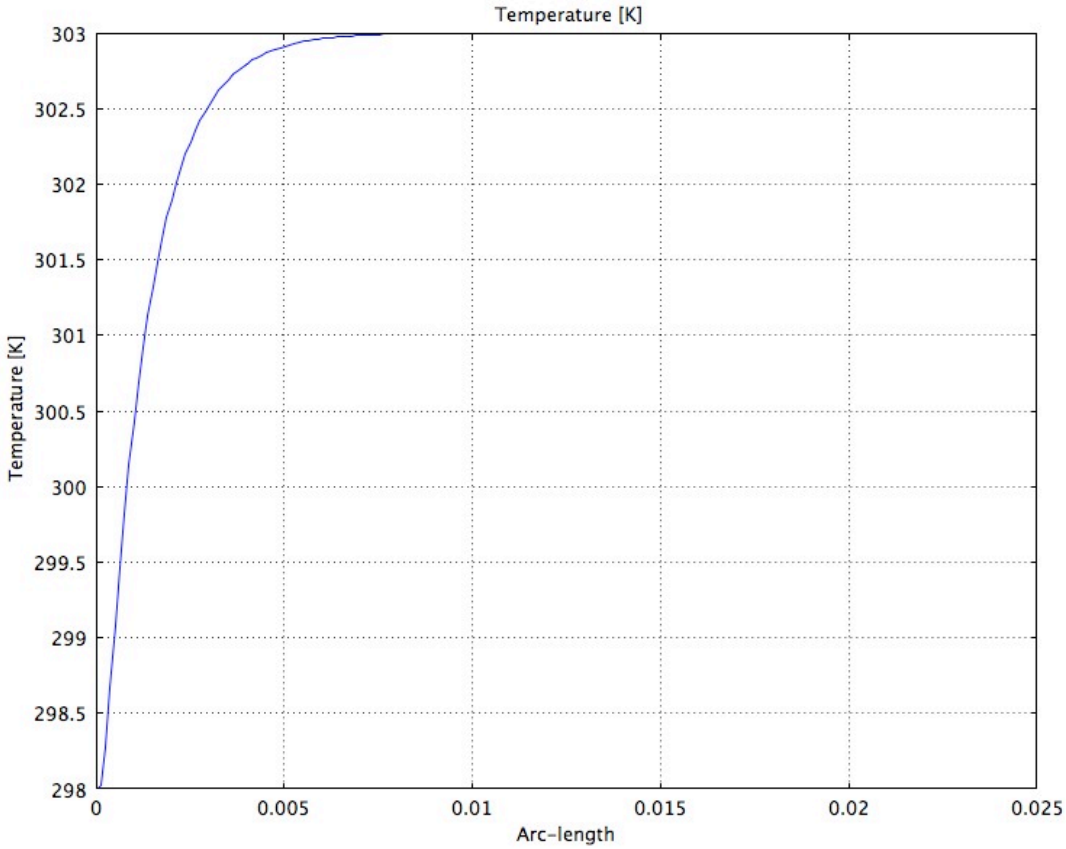

Figure 4. Centerline temperature

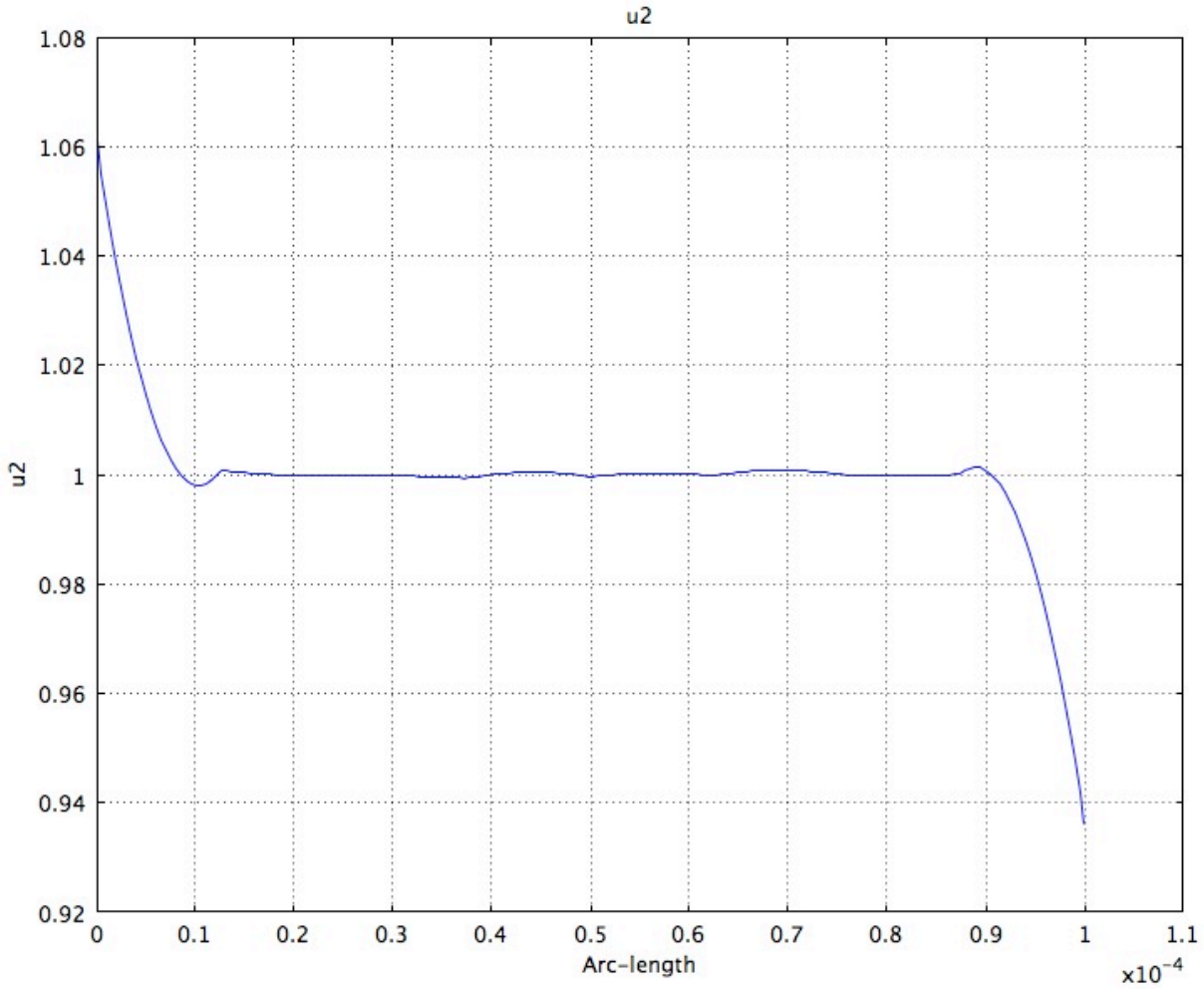

Figure 5. Relative mass fraction profile at outlet of TFFF, 76 mm

Transient TFFF

Next consider the same device but with no flow and in a transient mode. Now the problem is one-dimensional.

$$\rho C_p \frac{\partial T}{\partial t} = k\nabla^2 T, \quad \frac{\partial c}{\partial t} = \nabla \bullet [D\nabla c + D_T c \nabla T]$$

The top surface was taken at 308ºK, the bottom one at 298ºK, and the average mass fraction was taken as 1.0. This is a dimensionless value, the actual mass fraction divided by itself. Thus. the plots of mass fraction are relative mass fractions. The initial temperature was 298ºK and the initial relative mass fraction was 1.0. This problem was solved in Comsol Multiphysics, too, using the 1D option. There were 120 elements (equal lengths) with 482 degrees of freedom. Integration to 1000 seconds took only a few seconds on a Macintosh G5 computer. Since the boundary conditions on mass are no flux through the boundary (Neumann conditions), it is necessary to add another condition that sets the level of concentration. Otherwise a constant can

be added to the variable *c* and still satisfy the equation and boundary conditions. Here we keep the average concentration fixed, which is easily done in Comsol Multiphysics using the Integration Coupling Variables and a weak condition.

The temperature reached steady state in a very short time. The nominal time to reach steady state in a transient heat conduction problem is

$$t = \frac{L^2 \rho C_p}{k},$$

and that gives 0.0685 s, which was observed. Thus, it is really only necessary to calculate the mass fraction variation with time. The mass fraction profile as a function of time from 0 to 200 seconds is shown in Figure 6, and it is still changing. Calculating on to 1000 seconds shows that steady state has been reached, as shown in Figure 7. The mass fraction at the center as a function of time is shown in Figure 8, and steady state is reached in about 700-900 seconds.

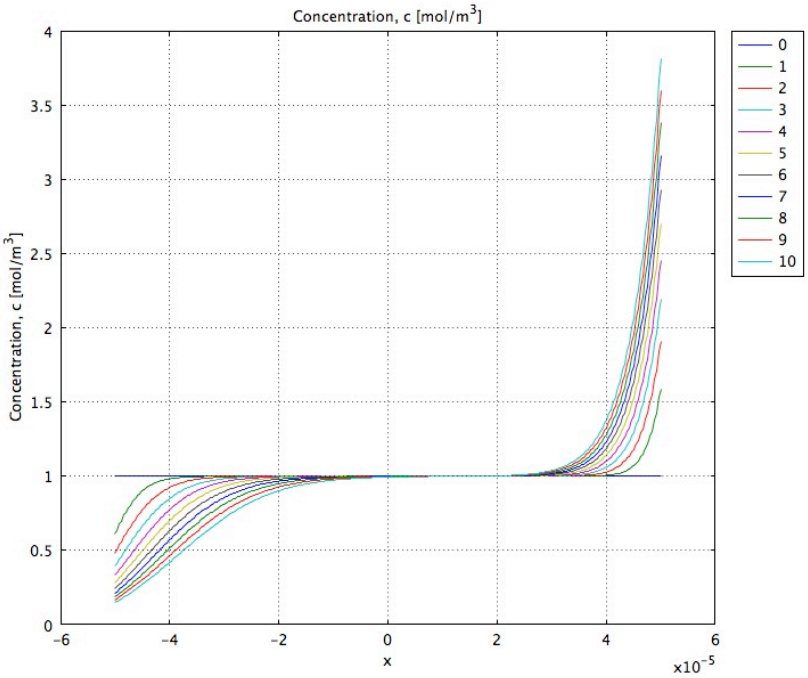

Figure 6. Solution for 100 ºC from t = 0 to 10 seconds

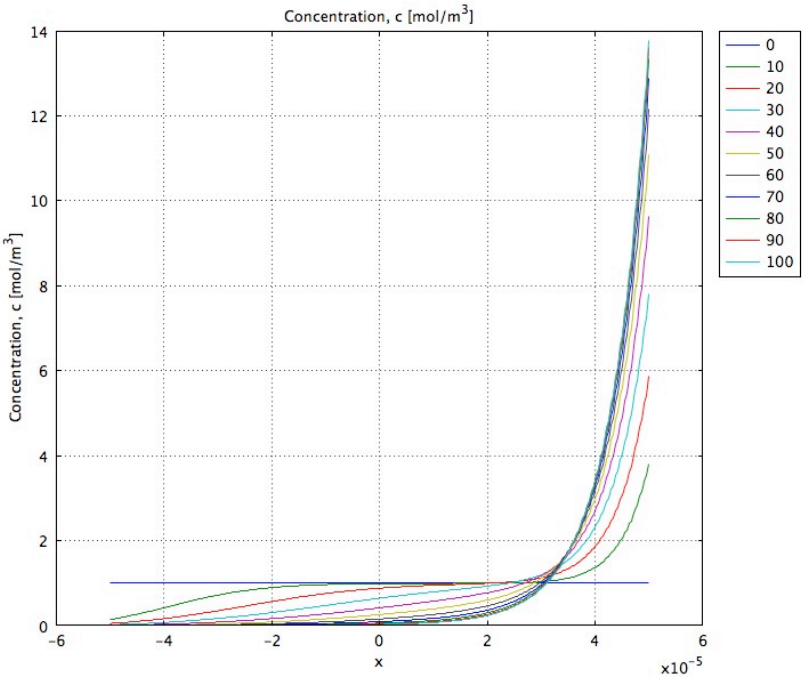

Figure 7. Solution for 100 ºC from t = 0 to 100 seconds

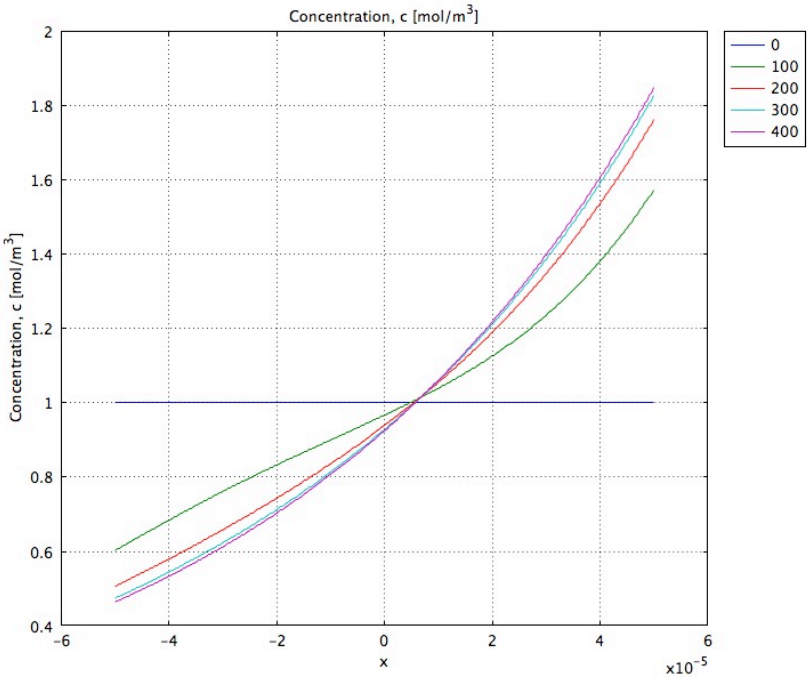

Figure 8. Solution for 10 ºC from t = 0 to 400 seconds

Convection with Thermal Diffusion

Consider next a thin cylinder of solution and solvent. A laser is used to heat a center core of the cylinder. This causes convection to occur due to density differences caused by temperature differences, and thermal diffusion can occur. This was shown experimentally for DNA by Braun and Libchaber (1). The goal here is to simulate this experiment of thermophoretic depletion and concentration.

The equations in this case are similar to those given above with two additions: a buoyancy term is added to the Navier-Stokes equation in the Boussinesq approximation, and a heat generation term is included in the energy equation. The power of the laser was assumed to be a Gaussian distribution about the center and uniform from top to bottom. Obviously, the experimental case is more complicated than this, but the exact power distribution is not known. Comsol Multiphysics was used to simulate this process as a function of time in axi-symmetric geometry. Since the domain is a closed vessel it is necessary to set the pressure at one point; it was set to zero at one point since it is determined only up to a constant anyway. Initially the temperature is uniformly room temperature and the relative mass fraction is uniformly 1.0.

Figure 9 shows the experimental situation of Braun and Libchaber (1). The DNA tends to collect on the bottom during the experiment, due to convection and thermal diffusion. Here we just provide qualitative information from the solutions. Figure 10 shows the relative mass fraction along the bottom surface, and it is clearly increasing in time. The distribution of mass fraction throughout the device is shown in Figure 11 and shows the same thing. The results are compared qualitatively with experiment in Figure 12, which shows the normalized concentration as a function of normalized time.

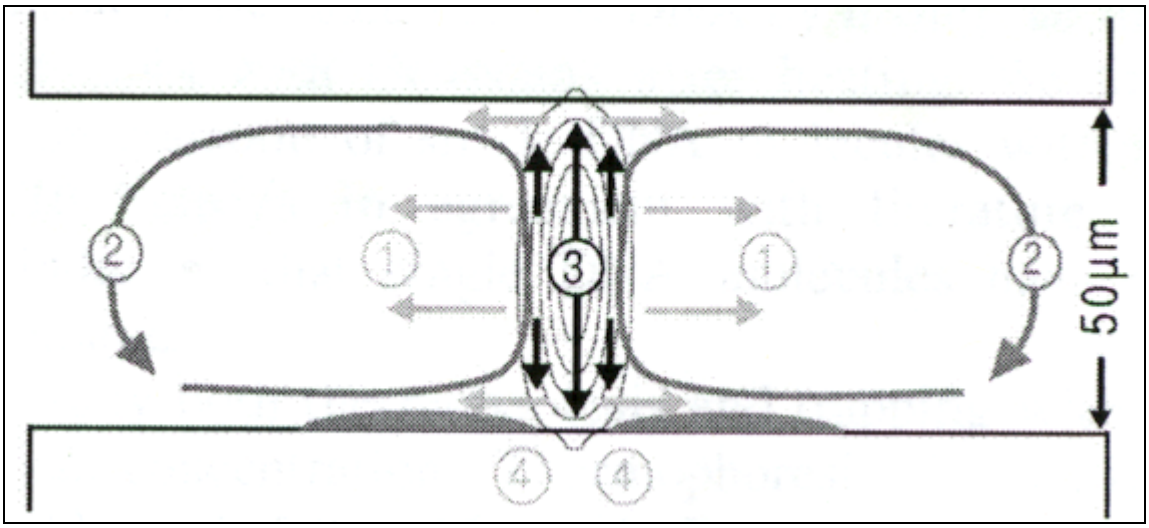

Figure 9. DNA chamber of the experiment reported by Braun and Libchaber (1)

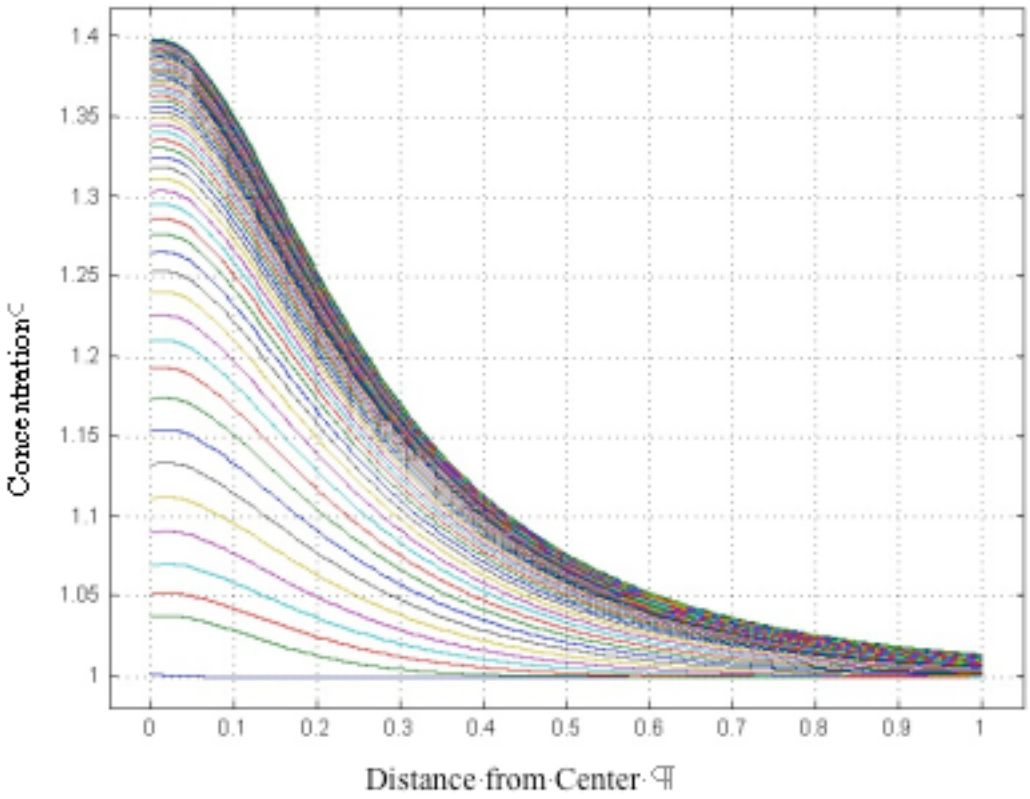

Figure 10. Relative mass fraction along bottom of chamber

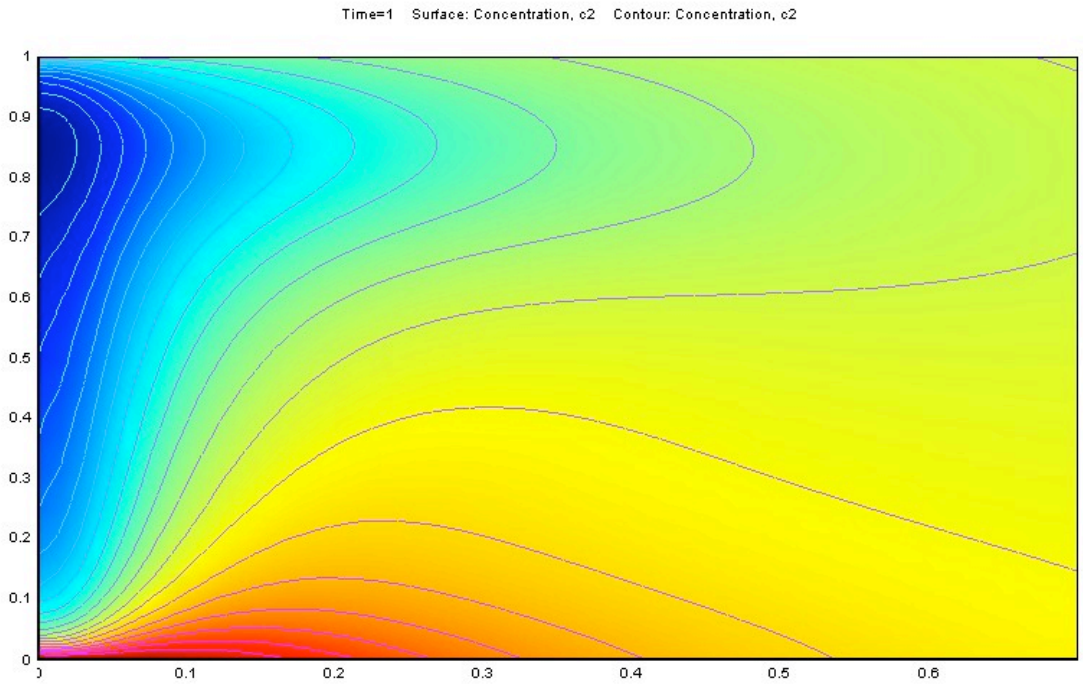

Figure 11. Relative mass fraction distribution at t = 5 seconds

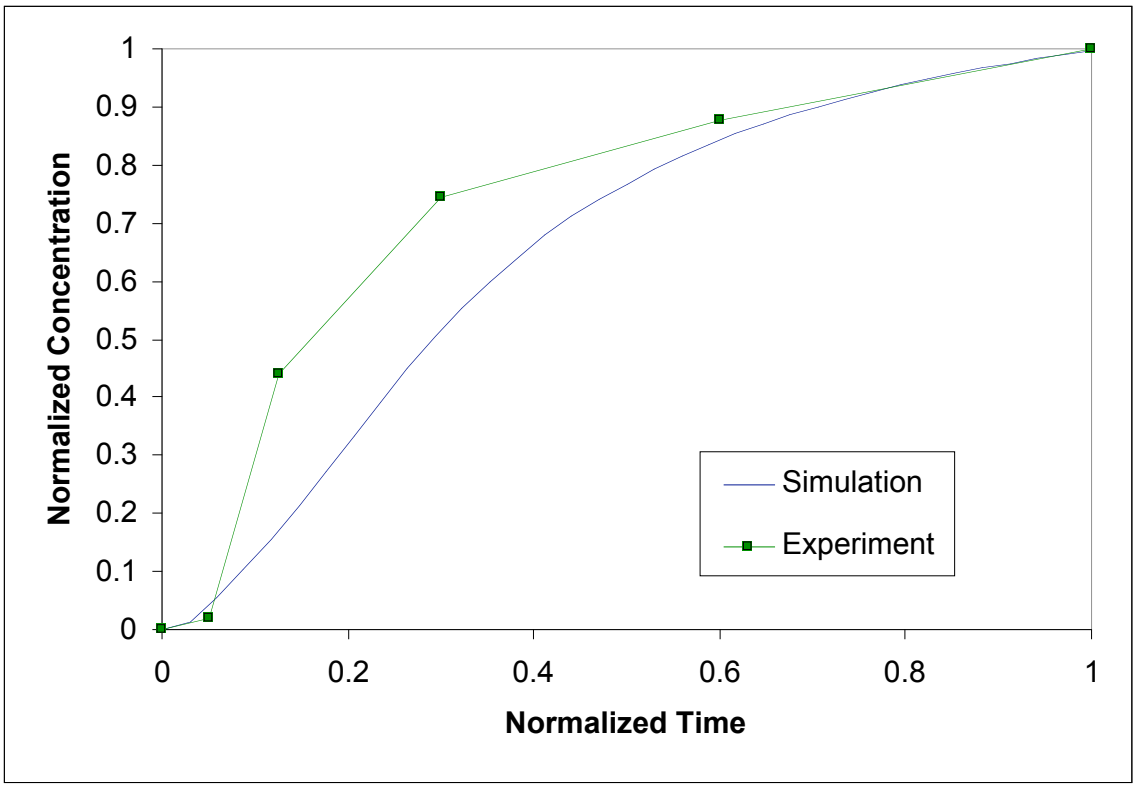

Figure 12. Normalized buildup of DNA along bottom of chamber

Conclusion

The simulations show that some transport effects can be neglected in thermal flow field fractionation devices: the development of the parabolic velocity profile and the constant vertical temperature gradient have little effect on the final results, especially in these long devices with a small aspect ratio. The mass fraction profile, though, develops more slowly and when there is flow it takes a long distance for it to reach its fully developed result.

The simulations of thermophoretic depletion and concentration show qualitative agreement with experiments reported in the literature.

Acknowledgement

Recent undergraduate projects have been supported by the Dreyfus Senior Mentor Award, which provides partial tuition payments to students doing undergraduate research.

References

1. Braun and Libchaber, (2002) "Trapping of DNA by Thermophoretic Depletion and Convection," *Phy. Rev. Letters*, **89**, 188103.
2. deGroot, S. R. and P. Mazur, (1954) *Non-Equilibrium Thermodynamics,"* Dover.
3. Brenner, H., (2006) "Elementary kinematical model of thermal diffusion in liquids and gases," *Phys. Rev. E*, **74** 036306-1-20.
4. Lenglet, J., A. Bourdon, J. C. Bacri, and G. Demouchy, (2002), "Thermodiffusion in magnetic colloids evidenced and studied by forced Rayleigh scattering experiments," *Phys. Rev. E*, **65** 031408-1-14.
5. Giddings, J. C., (1993) "Field-Flow Fractionation: Analysis of Macromolecular, Colloidal, and particulate Materials," *Science*, **260** 1456-1465.
6. Kreft, J. and Y.-L. Chan, (2007) "Thermal diffusion by Brownian motion induced fluid stress," *Phys. Rev. E,* **76** 021912-1-6.
7. Janca, J., (2006) "Micro-Thermal Field-Flow Fractionation in the Analysis of Polymers and Particles: A Review," *Int. J. Polymer Anal. Charact.,* **11** 57-70.